Photoinduced effects and holographic recording in amorphous $As_{100-x}Se_x$, As_2Se_3:Sn and Sb_2Se_3:Sn films

M. S. IOVU[*], D. V. HAREA, E. P. COLOMEICO, I. A. COJOCARU
Center of Optoelectronics of the Institute of Applied Physics, Academy of Sciences of Moldova,
Str. Academiei 5, MD-2028 Chisinau, Republic of Moldova

The optical and holographic characteristics of amorphous $As_{100-x}Se_x$, As_2Se_3:Sn and Sb_2Se_3:Sn prepared by vacuum evaporation on glass substrates are investigated. From the transmission spectra the changes of the refractive index under the light irradiation and heat treatment are calculated. . The band gap for amorphous Sb_2Se_3 was found to be E_g=1.30 eV and decrease with increasing of the tin concentration up to E_g=1.0 eV for Sb_2Se_3:$Sn_{10.0}$. The kinetics of photoinduced absorption and holographic recording in the investigated thin films was studied. The compositional and thickness dependences of the light induced optical parameters are determinate. The modifications of the refractive index under the light irradiation make these materials suitable for registration of optical and holographic information.

1. Introduction

Photo-structural transformations in amorphous films of chalcogenide glasses under light irradiation present a great fundamental interest for the establishment of the general legitimacy of interaction of the optical irradiation with the amorphous solids. The effect of light-induced photo-structural transformations is characteristic for many amorphous chalcogenides films, and have been initiated a lot of applications of amorphous material in photonics and optoelectronics, especially as inorganic photo-resists for sub-micron technology [1-3]. The interest in optical properties of amorphous semiconductors has been stimulated also by their possible applications as switching elements and optical fibers, as well as by their use as passivating materials for integrated circuits. Special interest for the applications of chalcogenide amorphous films is connected with doping with metal impurities, which alter optical, photoelectrical and transport properties of the host material [4-6]. At the same time it was shown that doping of chalcogenide films by tin impurities assist in stabilizing the glassy matrix with respect to light exposure and thermal treatment [7,8]. According to [119]Sn in the As_2Se_3:Sn glassy system according th the Mössbauer spectroscopy [8], new tetrahedral $Sn(Se_{1/2})_4$ and quasi-octahedral SnSe structural units can be formed, and which can influence the photostructural transformations. In this paper are presented the experimental results of optical transmission spectra of thermally evaporated thin films (thickness ~1.0÷3.0 μm) of $As_{100-x}Se_x$(x=40÷98), As_2Se_3:Sn_x and Sb_2Se_3:Sn_x (x=0÷10.0 at.%). The transmissions spectra are used for calculate the absorption coefficient, the optical band gap, as well as the dependence of the refractive index on composition, and its modifications under light irradiation and heat treatment. For the amorphous $As_{100-x}Se_{-x}$ the compositional and thickness dependences of the light induced optical parameters are determinate.

2. Experimental

The amorphous $As_{100-x}Se_x$, As_2Se_3:Sn_x and Sb_2Se_3:Sn_x (x=0÷10.0) thin films were obtained by "flash" thermal evaporation in vacuum (p=10[-5] Torr) of the initial synthesized material onto the clean glass substrates. The thickness of the films was about d~1÷3.0 μm. For optical transmission a UV/VIS (300÷800 nm) and 61 NIR (800÷3500 nm) Specord's CARLZEISS Jena production were used. The influence of the light exposure on the optical transmission was examined by illumination of the samples during 1 hour by light with the intensity F=50000 Lux. The thermal treating effect was examined by annealing of a part of the films in vacuum at T_{ann}=100 °C during one hour. After the annealing and light exposure the optical transmission was registered in the same manner.

In order to initiate the photostructural transformations in the thin film samples a red He-Ne (λ=0,63 μm, *P*=0.6 mW) and a green (λ=0,54 μm, *P*=0.75 mW) continuous lasers were used simultaneously as a sources of light exposure. The relaxation of the transmission curves was measured both at 0,63 μm and 0,54 μm wavelengths during the excitation. The laser spot on the sample was about 1 mm in diameter. The experimental set-up included a digital build-in PC-card for data acquisition PCI-1713A connected with the registration module. Fig. 1a and Fig. 1b represent the set-up for registration of the kinetics of the relaxation of the transmission curves and for registration

of the intensity of the first diffraction maxima during recording of the holographic gratings.
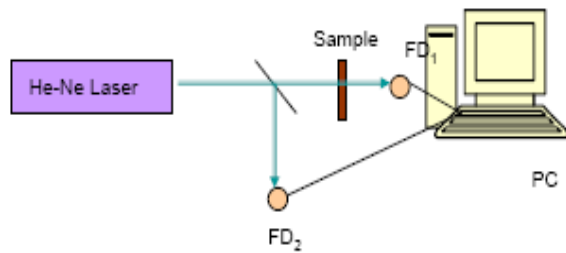

Fig.1a. The experimental set-up for measuring the optical transmittance during photodarkening
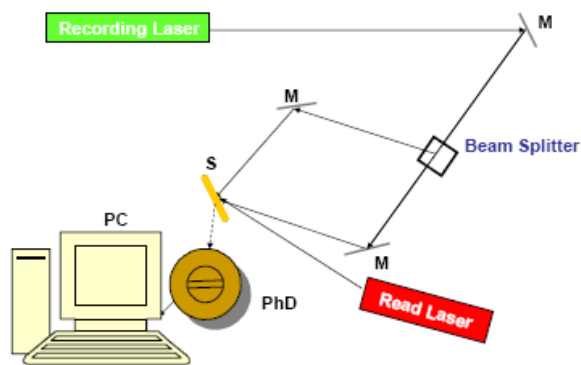

Fig.1b. The experimental set-up for recording of the holographic gratings.

3. Results and discussion

Fig.2a and Fig.2b show the transmission spectra for as-deposited amorphous As_2Se_3:Sn and Sb_2Se_3:Sn films. The optical transmission T for thin films is determined by the expression:

$$T = \frac{(1-R)^2 \exp(-kd)}{1 - R^2 \exp(-2kd)}, \qquad (1)$$

where R - is the optical reflection, k - the absorption coefficient, and d - the thickness of the amorphous film. In the visible region the reflection is constant and for calculations of the absorption coefficient was taken the value $R = 20$ %. The increasing of Sn concentration in amorphous As_2Se_3 and Sb_2Se_3 thin films shifts the absorption edge in the red region of the spectra and decreases the optical band gap.

In the consideration that the member $R^2 e^{-2\alpha d} \ll 1$ from the equation (1) we can obtain the expression for calculation of the absorption coefficient

$$\alpha = \frac{1}{d} \ln \frac{(1-R)^2}{T} \qquad (2)$$

The optical band gap E_g for as-deposited amorphous films was calculated from the relation:

$$(\alpha\, h\nu)^{1/2} = A(h\nu - E_g), \qquad (3)$$

where A − is a constant. A plot $(\alpha \cdot h\nu)^{1/2} \sim h\nu$ (Tauc plot) yields a straight line and the extrapolation of the photon energy axis $(\alpha \cdot h\nu)^{1/2} \to 0$ give the values of the optical band gap E_g.

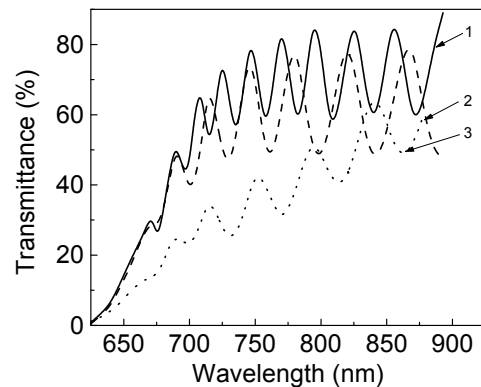*Fig.2a. The transmission spectra for as-deposited amorphous As_2Se_3 (1), As_2Se_3:Sn_{05} (2) and As_2Se_3:$Sn_{2.0}$ (3) thin films.*
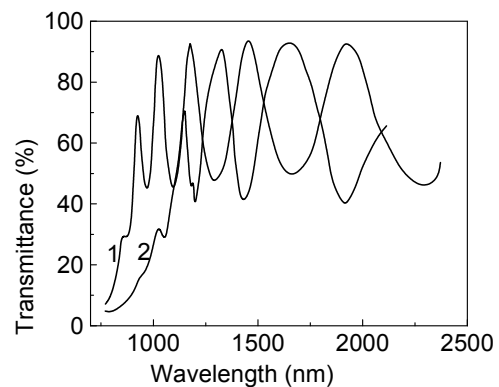
Fig.2b. The transmission spectra of amorphous Sb_2Se_3 (1, L=0.8μm) and Sb_2Se_3:$Sn_{10.0}$ (2, L=0.9 μm) thin films.

Increasing of the As content in the glass system As_xSe_{100-x} shift the absorption edge in the red region of the spectrum. This is in accordance with the experimental data obtained in [9], according which the band gap Eg decrease from E_g=1,95 eV for As_8Se_{92} up to E_g=1,83 eV for $As_{36}Se_{64}$. Increasing of the Sn concentration in the amorphous As_2Se_3:Sn films also decrease the optical band gap as was reported for the amorphous films AsSe:Sn [5]. The value of the optical band gap for amorphous Sb_2Se_3 films was obtained E_g=1.3 eV. This value for the optical band gap is in a good agreement with those obtained for the Sb_2Se_3 hollow nanospheres (E_g=1.33 eV) [10], and

other published data for amorphous Sb_2Se_3 films (E_g=1.25 eV). Increasing of Sn concentration in Sb_2Se_3 decrease the optical band gap, and for amorphous Sb_2Se_3:Sn_{10} films E_g=1.0 eV.

For the semiconductor transparent thin film the transmission spectra, when the thickness d is comparable with the wavelength λ represents the curve with interference maxima and minima. For normal incident light the dependence of transmission T vs. wavelength λ, the refractive index n and the thickness d mathematically can be expressed as [11]:

$$T = \frac{(1-R)^2}{1+R^2 - 2R\cos\delta}, \qquad (4)$$

were $\delta = \frac{4\pi}{\lambda}nd$ and $R = (\frac{n-1}{n+1})$.

From (4) follow that in the transparence region of the spectra at the wavelengths

$\lambda_{max} = \frac{4nd}{m}$, m=2, 4, 6, . . . we have the maximums, and

at the wavelengths $\lambda = \frac{4nd}{m}$, m=1, 3, 5, . . . we have the minimums.

Than for each λ_m and λ_{m-1}, corresponding to the neighbor extremes in the transmission spectra, we can calculate the refractive index n:

$$n = \frac{\lambda_m \lambda_{m-1}}{2d(\lambda_{m-1} - \lambda_m)} \qquad (5)$$

Fig. 3a shows a dependence of the refractive index n vs. wavelength λ for as-deposited and exposed amorphous $As_{60}Se_{40}$ thin films. Light exposure and heat treatment increase the refractive index n.
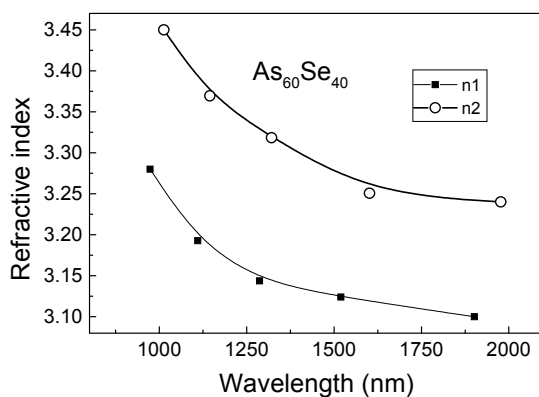

Fig.3a. The dependence of the refractive index n vs. wavelength for amorphous $As_{40}Se_{60}$ films before (n_1) and after (n_2) light exposure.

The photoinduced shift of the absorption edge $(\Delta\lambda)$ as well as the changes in the refractive index (Δn) depends at the fixed temperature depends on the exposure intensity, exposure time, film thickness, and on the composition of the amorphous thin film. The maximum shift of the absorption edge $\Delta\lambda$ at the level of transmittance T=20 % consists $\Delta\lambda$=920 nm, for $As_{60}Se_{40}$ films, while for $As_{10}Se_{90}$ and As_5Se_{95} films this value is only $\Delta\lambda$=2÷5 nm.
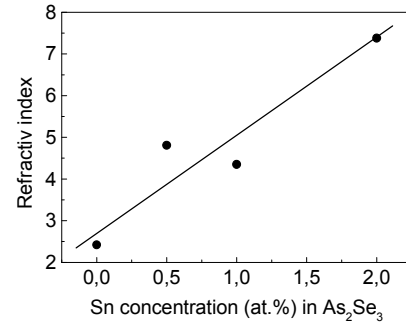

Fig.3b. The dependence of the refractive index vs. Sn concentration of amorphous $As_{40}Se_{60}$:Sn films (λ=720 nm).

In the same matter, the relative change of the refractive index $\Delta n/n$ is bigger for $As_{60}Se_{40}$ films ($\Delta n/n$=0.394) and decrease with increasing the concentration of Se in $As_{100-x}Se_x$ glassy system (Fig.4a and 4b). Our experimental data correlate with the experimental data for As-Se films obtained in [12,13].
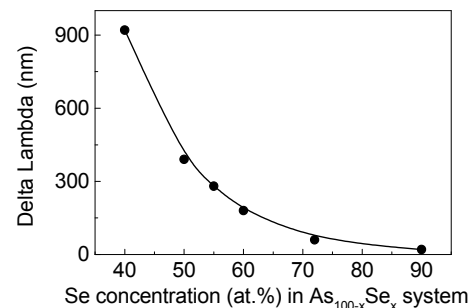

Fig. 4a.. The dependence of the photoinduced shifts of the absorption edge $(\Delta\lambda)$ versus Se content (at. %) in $As_{100-x}Se_x$ glass system.
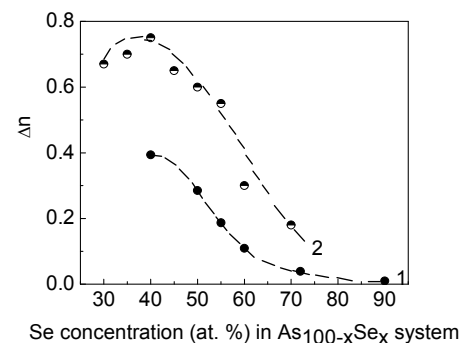

Fig.4b. The dependence of the relative changes of the refractive index Δn vs. Se content (at. %) in $As_{100-x}Se_x$ glass system. 1 – our data, 2 – after Ref. [13].

Fig. 5a shows the dependence of the refractive index n vs. wavelength λ for amorphous Sb_2Se_3 with different concentrations of tin. The refractive index depends on the Sn concentration in amorphous Sb_2Se_3 films, on light irradiation, and heat treatment. In the wavelengths region 1100÷2000 nm tin impurities (up to 0.5 at.% Sn) increase the refractive index, than for 10.0 at. % Sn, decrease. This may be due to the formation of new structural units, like SnSe and SnO_2. For small concentrations of tin (x=0.01 and 0.5 at.% Sn) illumination and heat treatment increase the refractive index n.
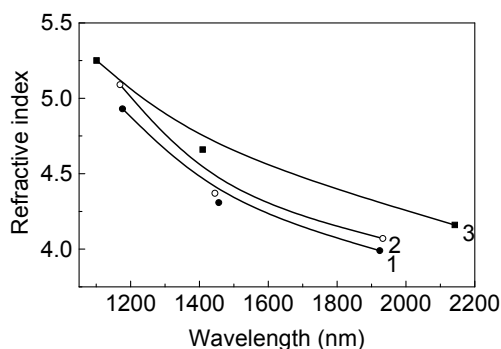

Fig.5a. The dispersion curves of the refractive index for amorphous Sb_2Se_3 (1), $Sb_2Se_3:Sn_{0.01}$ (2), and $Sb_2Se_3:Sn_{0.5}$ (3) thin films.
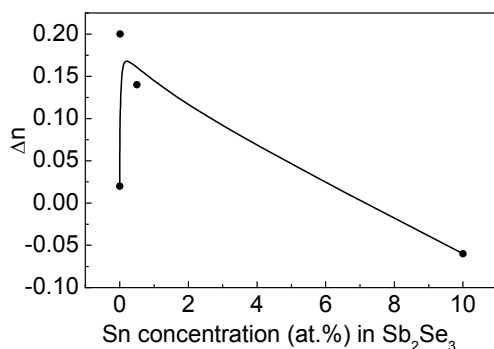

Fig.5b. Variation of the refractive index under the light exposure Δn vs. Sn concentration in amorphous Sb_2Se_3 thin films.

The maxima changes in the refractive index Δn (about Δn=0.20) occur for the composition $Sb_2Se_3:Sn_{0.01}$ and $Sb_2Se_3:Sn_{0.05}$. That allows us to conclude that doping of amorphous Sb_2Se_3 films with small concentrations of tin initiate the photostructural transformations under light irradiation, and make these materials suitable for registration of optical information. The similar effect was observed for the amorphous Sb-Se-In films. Increasing of In atoms in Sb-Se-In films improve the optical information recording characteristics [14]. Low concentrations of tin in Sb_2Se_3 increases under the light irradiation $(\Delta n > 0$, Fig.5b), i.e. the photodarkening effect take place. At the same time,

at high concentration of tin (10 at. % Sn) in Sb_2Se_3, the light irradiation decreases the refractive index ($\Delta n < 0$), i.e. changing the composition of the amorphous Sb_2Se_3 thin film using the different concentrations of tin impurities, we can create conditions for *"negative"*, as well as *"positive"* information recording process.

For the amorphous films $Sb_2Se_3:Sn_x$ the maximal modifications of the refractive index Δn (about Δn=0.20) occur for the composition $Sb_2Se_3:Sn_{0.01}$ and $Sb_2Se_3:Sn_{0.05}$. That allows us to conclude that doping of amorphous Sb_2Se_3 films with small concentrations of tin initiate the photo-structural transformations under light irradiation, and make these materials suitable for registration of optical information.

Photodarkening relaxation was measured during illumination for amorphous $As_{100-x}Se_x$ (x=40÷98), for as-deposited and annealed films at T_{ann}=120 ^oC during 1 hour. The relaxation of the relative optical transmission $T(t)/T(0)$ of the amorphous $As_{60}Se_{40}$ films of different thickness is shown in Fig.6a. The experimental data show that for the thicker films the photodarkening is stronger, and almost is absent for the films with thickness about 0.2-0.3 μm. The influence of the thickness on the photodarkening effect was also investigated for the amorphous As_2S_3 and As_2Se_3 films [15], and for As_2Se_3 pure and doped with Dy and Pr films [16].
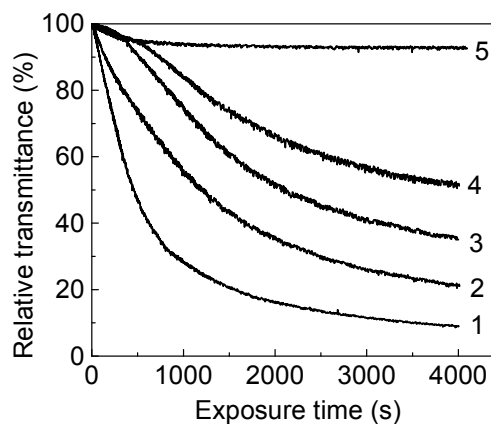

Fig.6a. The dependence of transmission versus exposure time for amorphous $As_{60}Se_{40}$ films of different thickness L, μm 1-4.07; 2-2.04; 3-0.76; 4-0.54; 5-0.27.

For the stoichiometric films irradiated by band gap illumination at room temperature was found that the photodarkening disappears when the films are thinner than 50 nm [17]. The authors explain this anomaly by the fact that the structure of the film is dependent on the film thickness either that the photodarkening exhibits a surface behaviour, which is different from bulk behaviour. On the other hand, a small photodarkening was observed in ·α-As_2Se_3 films of 30 nm in thickness [15]. According to [15] the thickness dependence of the photodarkening is based on the thickness dependence of the initial optical absorption edge before irradiation with band gap light. The authors explain the absence of photodarkening in thinner

films by the strain induced by the lattice mismatch between the film and the substrate.
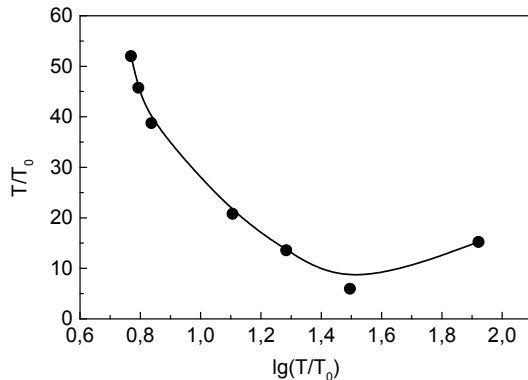

Fig.6b. The thickness dependence of the photodarkening in amorphous $As_{60}Se_{40}$ films.

According to transmission spectra measurements and to the results obtained in [16], we suggest that the thickness dependence of photodarkening is caused by different light amount absorbed in the film for different thickness, and which regulate the number of absorbed photons generating the photodarkening effect. The thickness dependence of photodarkening, presented in the coordinates T/T_0 vs. $lg(T/T_0)$ according [12] represent a curve with minimum (Fig.6b). For amorphous $As_{60}Se_{40}$ composition the maximum sensitivity is obtain for the films with the thickness of $L=4.0$ μm. Fig.7a shows the relaxation of the optical transmittance during illumination of as-deposited and annealed $As_{100-x}Se_x$ thin films. Increasing of Se content in $As_{100-x}Se_x$ thin films decrease the photodarkening, and this process is very small in the films with high content of Se. Fig.7b represents the relaxation of the optical transmittance during illumination of as-deposited $As_{40}Se_{60}$ thin films at two different intensities of Ne-He (λ=0.63 μm) laser beam. Decreasing of intensity of the incident light influence the kinetics of photodarkening at longer exposure times (curve 2). Some photoinduced effects in antimony containing amorphous films were investigated in [18,19]. In amorphous Sb_2S_3 and Sb_2Se_3 it was observed the optically induced crystallization and amorphization with the power threshold of 100-200 W/cm^2 [18]. From the Raman spectra investigations it was shown that the photoinduced changes of the structure are accompanied by changes of chemical bonds and the changes of atomic structure [20-22].

Fig.8a shows the kinetics of photodarkening in amorphous Sb_2Se_3 thin films doped with different concentrations of tin exposed with LED at 850 nm (W=1 mW). The undoped Sb_2Se_3 films exhibit small changes of transmittance under light exposure. Adding of Sn in amorphous Sb_2Se_3 increases the photostructural transformations under light irradiation, and reaches the maximum value for the composition Sb_2Se_3:$Sn_{0.05}$ (Fig.8b). Tease results are in good agreement with those obtained from the transmission spectra, according which the maximum changes of the refractive index Δn under the

light irradiation (about Δn=0.20) occur for the composition Sb_2Se_3:$Sn_{0.01}$ and Sb_2Se_3:$Sn_{0.05}$ (Fig.5b).

In our previous publications [7,8] it was shown that the observed relaxation of photodarckening is described by the stretched exponential function $T(t)/T(0) = A_0+Aexp[-(t-t_0)/\tau]^{(1-\alpha)}$, where t is the exposure time, τ is the apparent time constant, A characterizes the exponent amplitude, t_0 and A_0 are the initial coordinates, and α is the dispersion parameter $(0<\alpha<1)$.
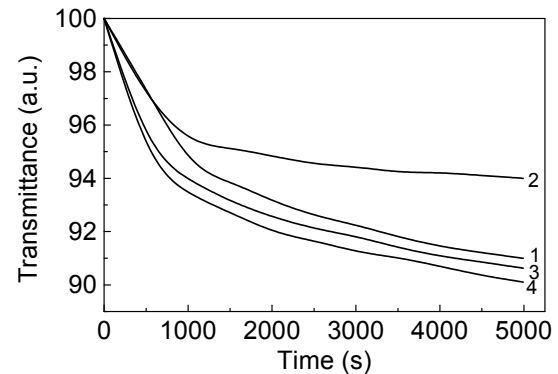

Fig.7a. Photodarkening kinetics of as-deposited amorphous $As_{40}Se_{60}$ (1), $As_{45}Se_{45}$ (2), $As_{50}Se_{50}$ (3), and $As_{60}Se_{40}$ (3) thin films. The transmission is measured at λ=0.54 μm.
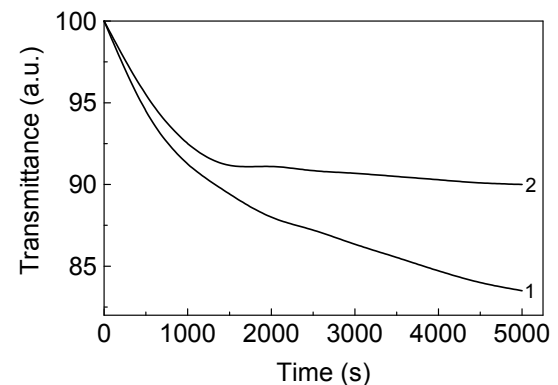

Fig.7b. Photodarkening kinetics of as-deposited amorphous $As_{40}Se_{60}$ measured at two different intensities of Ne-He (λ=0.63 μm) laser beam.

The fact that the photodarkening kinetics may be described by a stretched exponential we may consider as indication of dispersion in kinetic mechanism, i.e. the time dependence of the process rate. The data allow concluding that formation of photoinduced absorption is limited by a dispersive process with the exponent $\alpha \cong 0.5$. In our case it is the dispersive character of hole transport that may cause the dispersive character of the relaxation after photogeneration. The transport of photoexcited holes is included in the "slip motion" model for photodarkening in the stage when the layer clusters are charged due to capture of charge carriers [23]. This model was used by us

to explain the experimental results for amorphous As_2Se_3 films doped with tin [7,8] and rare-earths ions [24].
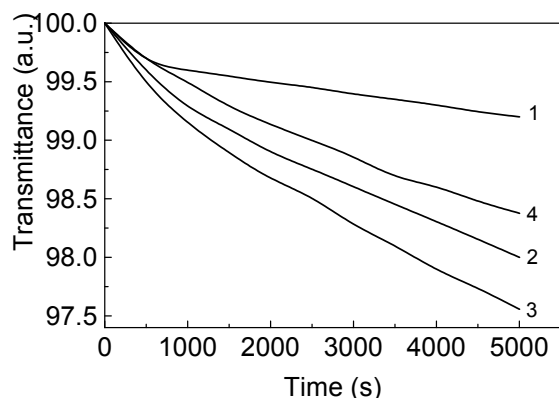

Fig.8a. Photodarkening kinetics of as-deposited amorphous Sb_2Se_3 (1), Sb_2Se_3:$Sn_{0.01}$ (2), Sb_2Se_3:$Sn_{0.05}$ (3), and Sb_2Se_3:$Sn_{10.0}$ (3) thin films. The transmission is measured at $\lambda=0.85$ μm.

Charge transport in chalcogenide glasses is known as highly dispersive due to wide distribution of capture times in multiple-trapping process [25,26].
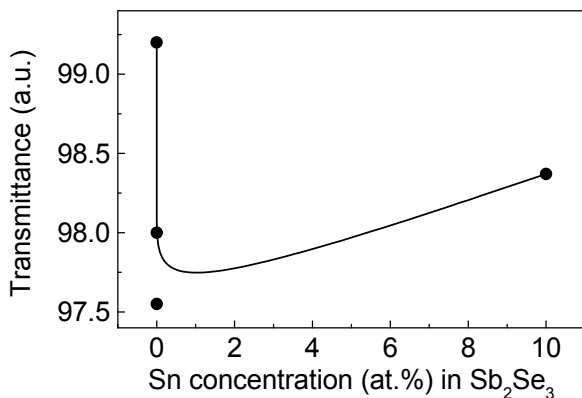

Fig.8b. The dependence of the photodarkening effect vs. Sn concentration in amorphous Sb_2Se_3 thin films.

For glasses like a-As_2Se_3 the dispersive parameter α of hole transport is close to 0.5, in accordance with the value found from the stretched exponential presentation of photodarkening kinetics. The fact that α is increasing in the Se-rich compositions indicates to the increasing of the ordering in the structure of amorphous films. The composition dependence of photodarkening may be caused by the different ratio of homopolar chemical bonds (As-As, Se-Se) and heteropolar (As-Se) in investigated amorphous films, and which are responsible for the photodarkening [27,28].
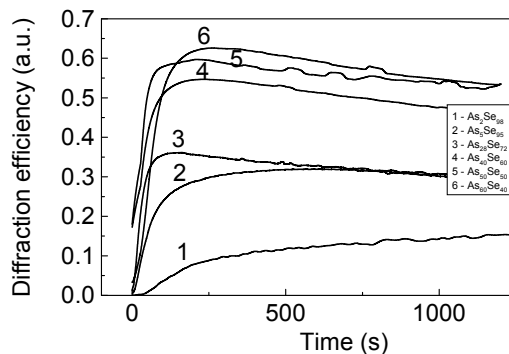

Fig.9a. The kinetics of growth of the diffraction efficiency vs. exposure time for amorphous films in the glassy system $As_{100-x}Se_x$.

The main functional principles and practical application of amorphous chalcogenide registration media for production of holograms and holographic diffraction elements are discussed in the papers of J.Teteris [13,29,30]. It was shown that the amorphous chalcogenide films (As.S, As-Se, As-S-Se) are one of the promising media for optical recording of holographic information with high diffraction efficiency and high resolution, Bragg grating structures and waveguides for integrated optics. In this paper we show that the amorphous films under study $As_{100-x}Se_x$, As_2Se_3:Sn and Sb_2Se_3:Sn exhibit high refractive index and it considerable modifications under light exposure. For this purpose we have investigated the process of recording of holographic gratings in the amorphous film of the glassy system $As_{100-x}Se_x$ and the thicknes dependence in one of more sensitive composition $As_{60}Se_{40}$.
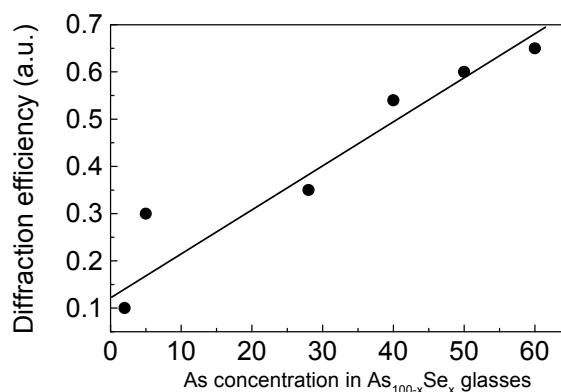

Fig.9b. The dependence of the diffraction efficiency vs. As concentration in the amorphous films of the glassy system $As_{100-x}Se_x$.

The kinetics of growth of the diffraction efficiency was investigated during exposure of two He-Ne laser beams ($\lambda=6328$ nm) with a power of $W=30$ mW. The

intensity of the first interference maximum was recorded in the transmittance mode.
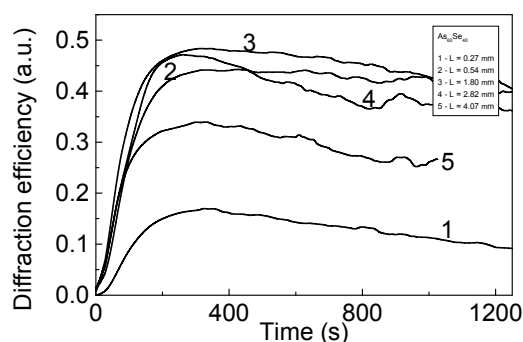

Fig.10a. The kinetics of growth of the diffraction efficiency vs. exposure time for amorphous $As_{60}Se_{40}$ films on different thickness.

Fig.9a represents the curves of growth of the diffraction efficiency during time exposure for different compositions of amorphous films in the glassy system $As_{100-x}Se_x$. Increasing of the As content in $As_{100-x}Se_x$ films accelerate the recording process and increase the diffraction efficiency.
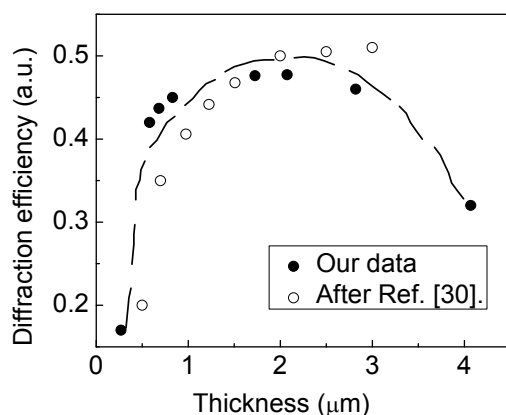

Fig.10b. The thickness dependence of the diffraction efficiency for amorphous $As_{60}Se_{40}$ thin films. 1 – our data, 2 – after Ref. [30] for the $As_{33}Se_{45}$ thin films.

The maximum value of the diffraction efficiency was recorded for the composition $As_{60}Se_{40}$ (Fig.9b). As we can see from the Fig.9a, the kinetics of the diffraction efficiency represents a curve with a maximum. The same dependence for the amorphous As_2S_3 and As-S-Se was observed in [13]. At the same time for the amorphous films $As_{100-x}S_x$ the maximum diffraction efficiency was recorded for the composition $As_{55}Se_{45}$ [30].. The Sn impurities in $As_{40}Se_{60}$ reduce the photodarkening effect and stabilizes the value of the diffraction efficiency, due to more rigid glass network [8,31].

The holographic sensitivity of the amorphous film depends on the recording wavelength, intensity and polarization of the laser beam and thickness of the layer. Fig.10a shows the kinetics of growth of the diffraction efficiency versus time exposure for amorphous $As_{60}Se_{40}$ films on different thickness. This dependence represents a curve with maximum corresponding to the value of film thickness of about d=2000 nm (Fig.10b), and are in good agreement with the experimental results obtained in [30]. The maximum value for the photodarkening process for this glass composition was obtained for the thickness of about d=1500 nm (Fig.6b).

5. Summary

The optical absorption spectra of amorphous $As_{100-x}Se_x$, As_2Se_3:Sn and Sb_2Se_3:Sn thin films were used in order to determine the optical band gap and the refractive index. The modifications of the refractive index under the light exposure and heat treatment also were investigated. It was shown that tin increase the photostructural transformation in the amorphous films under study. It was established, that the higher sensitivity to light exposure exhibit the non-stoichiometric $As_{50}Se_{50}$, $As_{55}Se_{45}$, and $As_{60}Se_{40}$ amorphous films, and decrease with increasing of Se content in the $As_{100-x}Se_x$ glass. The experimental results are interpreted in terms of structural optical polymerization process, which includes the transformation of As_4Se_4 and Se_2 structural units in homogenius $AsSe_{3/2}$ network. According to ^{119}Sn in the As_2Se_3:Sn glassy system according th the Mössbauer spectroscopy [8], new tetrahedral $Sn(Se_{1/2})_4$ and quasi-octahedral SnSe structural units can be formed, and which can influence the photostructural transformations. For the Sb_2Se_3:Sn, in dependence of the composition of the amorphous thin films the "photodarkening" and "photobleaching" effects were established. On the basis of investigations of the photodarkening effect and holography recording of the diffraction gratings in $As_{100-x}Se_x$ was established the thickness dependence, the maximum sensitivity which occurs at about 2 μm of thickness. The obtained experimental results allow us to conclude, the amorphous amorphous $As_{100-x}Se_x$, As_2Se_3:Sn and Sb_2Se_3:Sn thin films are perspective for registration of holography information.

References

[1] A. M.Andriesh, M. S. Iovu, In Series; Optoelectronic Materials and Devices, V.1, 2004, Non-Crystalline Materials for Optoelectronics, Eds. G.Lucovsky & M. Popescu, INOE Publishing House, Bucharest,

p.155 (2004).

[2] A. Andriesh, S. Sergheev, G. Triduh, A. Meshalkin, J. Optoelectron. Adv. Mater. **9**, 3007 (2007).

[3] A. Gerbreders, J. Teteris, J. Optoelectron. Adv. Mater. **9**, 3164 (2007).

[4] M. S. Iovu, S. D. Shutov, L. Toth, Physica Status Solidi (b), **195**, 149 (1996).

[5] M. S. Iovu, N. N. Syrbu, S. D. Shutov, I. A. Vasiliev, S. Rebeja, E. Colomeico, M. Popescu, F. Sava, Physica Status Solidi (a), **175**, 615 (1996).

[6] M. S. Iovu, S. D. Shutov, V. I. Arkhipov, G. J. Adriaenssens, J. of Non-Cryst. Solids **299&302**, 1008 (2002).

[7] M. S. Iovu, S. D. Shutov, M. Popescu, J. of Non-Cryst. Solids **299&302**, 924 (2002).

[8] P. Boolchand, D. G. Georgiev, M. S. Iovu, Chalcogenide Letters **2**, 27 (2005).

[9] P. Nagels, Romanian Reports in Physics **51**, 209 (1999).

[10] Z. Yunxia, L. Guanghai, Z. Bo, Z. Lide, Materials Letters **58**, 2279 (2004).

[11] Yu. I. Uhanov, Optical properties of semiconductors, Ed. V.M.Tuchkevich, NAUKA, Moscow, 1977 (In Russian).

[12] V. M. Lyubin, Photographical process on the base of Vitreous Chalcogenide glasses. In the Book: NON-SILVER PHOTOGRAPHICAL PROCESSES, Edited by A.L.Kartujanskii, Chimia, Leningrad, pp. 193-215, 1984 (in Russian).

[13] J.Teteris, J. Optoelectron. Adv. Mater. **4**, 687 (2002).

[14] V. M. Rubish, P. P. Shtets, V. V.Rubish, D. G. Semak, B. R. Tsizh, J. Optoelectron. Adv. Mater. **5**, 1193 (2003).

[15] K. Hayashi, N. Mitsuishi, J. of Non-Cryst. Solids **299&302**, 949 (2002).

[16] M. S. Iovu, S. D. Shutov, P. Boolchand, E. P. Colomeico, V. G. Ciorba, S. M. Iovu, M. Popescu., J. Optoelectron. Adv. Mater. **4**, 857 (2002).

[17] K.Tanaka, S.Kyohya, A.Odajima, Thin Solid Films **111**, 195 (1984).

[18] P. Arun, A. G. Vedeshwar, N. C. Mehra, J. Phys. D, Appl. Phys. **32**, 183 (1999).

[19] T. Aoki, H. Shimada, N. Hirao, N. Yoshida, K. Shimakawa, S. R. Elliot, Phys. Rev. **B59**, 1579 (1999).

[20] M. Frumar, A. P. Firth, A. E. Owen, J. Non-Cryst. Sol. **192&193,** 447 (1995),

[21] M. S. Iovu, S. D. Shutov, A. M. Andriesh, E. I. Kamitsos, C. P. E. Varsamis, D. Furniss, A. B. Seddon, M.Popescu, J. Optoelectron. Adv. Mater. **3**, 443 (2001).

[22] M. S. Iovu, E. I. Kamitsos, C. P. E. Varsamis, P. Boolchand, M. Popescu, J. Optoelectron. Adv. Mater. **7**, 763 (2005).

[23] K. Shimakawa, N. Yoshida, A. Ganjoo, Y. Kuzukawa, J. Singh, Phil. Mag. Letters **77**, 153 (1998).

[24] M. S. Iovu, P. Boolchand, D. G. Georgiev, J. Optoelectron. Adv. Mater. **7**, 763 (2005).

[25] H.Scher, E.W.Montroll, Phys. Rev. **B12**, 2455 (1975).

[26] G. Pfister, H.Scher, Phys. Rev. **B15**, 2062 (1977).

[27] M. Frumar, A.F.Firth, A.E.Owen, J. of Non-Cryst. Solids **59&60**, 921 (1983).

[28] O. I. Shpotyuk, Opto-Electronics Review **11**, 19 (2003).

[29] J.Teteris, M.Reinfelde, J. Optoelectron. Adv. Mater. **5**, 1355 (2003).

[30] J. Teteris, M. Reinfelde, J. Optoelectron. Adv. Mater. **7**, 2581 (2005).

[31] A. I. Buzdugan, M. S. Iovu, A. A. Popescu, P. G. Cerbari, Balkan Physics Letters **1**, 7 (1993).

———————————
*Corresponding author: miovu@asm.md